# Dielectric Elastomer Generators: How Much Energy Can Be Converted?

Soo Jin Adrian Koh, Christoph Keplinger, Tiefeng Li, Siegfried Bauer, *Senior Member, IEEE*, and Zhigang Suo

***Abstract*—Dielectric elastomers are being developed as generators to harvest energy from renewable sources, such as human movements and ocean waves. We model a generator as a system of two degrees of freedom, represented on either the stress–stretch plane or the voltage–charge plane. A point in such a plane represents a state of the generator, a curve represents a path of operation, a contour represents a cycle of operation, and the area enclosed by the contour represents the energy of conversion per cycle. Each mechanism of failure is represented by a curve in the plane. The curves of all the known mechanics of failure enclose the region of allowable states. The area of this region defines the maximum energy of conversion. This study includes the following mechanisms of failure: material rupture, loss of tension, electrical breakdown, and electromechanical instability. It is found that natural rubber outperforms VHB elastomer as a generator at strains less than 15%. Furthermore, by varying material parameters, energy of conversion can be increased above 1.0 J/g.**

***Index Terms*—Dielectric materials, energy conversion, generators, modeling.**

## I. INTRODUCTION

A MEMBRANE of a dielectric elastomer, sandwiched between two compliant electrodes, is a deformable capacitor (see Fig. 1). Subject to a voltage, the elastomer reduces its thickness and expands its area. Dielectric elastomers are being developed as actuators, converting changes in voltage to a deformation of the elastomer [1]–[8]. On the other hand, for a prestretched and precharged elastomers under open-circuit con-

S. J. A. Koh is with the School of Engineering and Applied Sciences, Harvard University, Cambridge, MA 02138 USA, and also with the Institute of High Performance Computing, Singapore 138632 (e-mail: asjkoh@seas.harvard.edu).
C. Keplinger is with the School of Engineering and Applied Sciences, Harvard University, Cambridge, MA 02138 USA, and also with the Soft-Matter Physics Department, Johannes Kepler University Linz, A-4040 Linz, Austria (e-mail: Christoph.Keplinger@jku.at).
T. Li is with the Institute of Applied Mechanics, Zhejiang University, Hangzhou 310027, China.
S. Bauer is with the Soft-Matter Physics Department, Johannes Kepler University Linz, A-4040 Linz, Austria (e-mail: Siegfried.Bauer@jku.at).
Z. Suo is with the School of Engineering and Applied Sciences, Harvard University, Cambridge, MA 02138 USA (e-mail: suo@seas.harvard.edu).
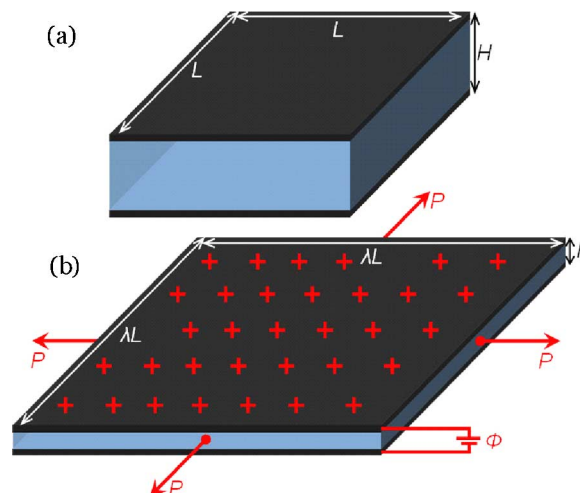
Fig. 1. Operation of a dielectric elastomer transducer. A membrane of a dielectric elastomer is sandwiched between compliant electrodes. (a) In the reference state, the membrane is subject to neither force nor voltage and is undeformed. (b) In the activated state, the membrane is subject to an equal-biaxial force $P$ in its plane and a voltage $\Phi$ through its thickness. The membrane expands the area by a factor of $\lambda^2$ and reduces the thickness from $H$ to $h$. Electrons flow through the external circuit, resulting in electric charges $\pm Q$ on the two electrodes.

ditions, a reduction of the tensile force thickens the membrane and increases the voltage. The process boosts electric charges from a low-voltage source to a high-voltage reservoir. In this case, the elastomer is used as a generator, converting the deformation of the elastomer to electrical energy.

Dielectric elastomer generators are being developed for both small-scale energy scavenging [9]–[11] and large-scale energy generation [12]. Unlike piezoceramics [13], [14], the technology has the potential to harvest energy from ocean waves. Elastomers are highly stretchable, enabling excellent force coupling. The efficiency of electromechanical conversion of elastomers is high [15]. Elastomers, such as natural rubber (NR), have been used in oceans and other harsh environments for well over a century. NR, polyacrylate VHB 3M, poly (dimethylsiloxane) PDMS, and other dielectric elastomers are available at low cost. These attributes may translate to lightweight, low-maintenance, and low-cost dielectric elastomer generators.

Existing experiments on dielectric elastomer generators usually restrict strains of operation well below 100%, with a frequency of excitation under 1 Hz, and report energy of conversion below 0.1 J/g [10], [11]. In one particular experiment [11], an energy of conversion of 0.028 J/g was achieved on a silicone dielectric elastomer, with a strain of operation of 15%. Even under such moderate strains of operation, the elastomer generators may be attractive alternatives to piezoceramics and

ferromagnets, because dielectric elastomers have desirable attributes, such as lightweight, low maintenance, and low cost. Furthermore, if larger strains of operation are permitted, a larger energy of conversion is possible.

This paper investigates the potential of dielectric elastomer generators for the full range of strain of operation. Following previous studies [16], [17], we calculate the maximum energy of conversion for dielectric elastomers on the basis of well-established mechanisms of failure: electrical breakdown, electromechanical instability (or pull-in instability), loss of tension, and material rupture [16]–[20]. The previous studies assumed the neo-Hookean stress–strain relation and a strain-independent electrical breakdown field. In this paper, we will invoke a stress–strain relation that captures stiffening due to the extension limit of polymer chains [21], [22]. We will also incorporate the experimental finding that the electrical breakdown field is enhanced by strain [19], [23], [24]. The method is used to compare the VHB elastomer with NR. When the strain of operation varies from 1% to 500%, the energy of conversion spans at least two orders of magnitude. NR outperforms VHB as a generator at strains less than 15%. The method also shows that the energy of conversion can be substantially increased by the development of new elastomer materials with varied material properties, such as elastic modulus, permittivity, and electrical breakdown field.

## II. EQUATIONS OF STATE AND MECHANISMS OF FAILURE

The performance of a dielectric elastomer transducer depends on its configuration. A relatively simple configuration is used here to illustrate the method of calculation. In the state of reference [see Fig. 1(a)], a membrane of a dielectric elastomer is undeformed and uncharged. In an activated state [see Fig. 1(b)], the elastomer is subject to an externally applied equal biaxial force $P$ in its plane and a voltage $\Phi$ through its thickness. Electrons flow through the external circuit, resulting in electric charges $\pm Q$ on the two electrodes. The elastomer stretches by $\lambda$ in both in-plane directions and reduces its thickness from $H$ to $h$. The elastomer is taken to be incompressible, so that $h = H\lambda^{-2}$. This analysis ignores dissipative effects, such as viscoelasticity, dielectric relaxation, and electrical conduction through the elastomer.

We regard the transducer as a system of four state variables: $P, \lambda, \Phi, Q$. These state variables are connected by equations of state, as described earlier. By definition, the electric displacement is $D = Q/(\lambda L)^2$, and the electric field is $E = \Phi/h = \Phi\lambda^2/H$. The electric displacement relates to the electric field as $D = \varepsilon E$, where $\varepsilon$ is the permittivity of the elastomer, taken to be a constant independent of the stretch [24]. A combination of these relations is written as

$$Q = \frac{\varepsilon L^2 \lambda^4}{H} \Phi. \tag{1}$$

This equation characterizes the transducer as a deformable capacitor. The factor in front of the voltage is the capacitance, which is proportional to $\lambda^4$. This strong dependence on the stretch results from both the expansion in area and reduction in thickness.

By definition, the nominal stress is $s = P/(LH)$. In the deformed state, the cross-sectional area of the membrane is $(\lambda L)\left(\lambda^{-2}H\right) = \lambda^{-1}LH$, so that the true stress is related to the nominal stress as $\sigma = \lambda s$. In the absence of a voltage, the nominal stress relates to the stretch as $s = F(\lambda)$. The function $F(\lambda)$ characterizes the elasticity of the elastomer, to be specified later. In the absence of a force $P$, when the elastomer is subject to an electric field $E$ through its thickness, the elastomer reduces thickness, and expands in area. The deformation caused by the electric field is identical to that caused by an equal-biaxial true stress of magnitude $\varepsilon E^2$, known as Maxwell stress [25]. This equal-biaxial true stress is equivalent to an equal-biaxial nominal stress $\varepsilon E^2 \lambda^{-1}$, which is expressed as $\varepsilon \left(\Phi/H\right)^2 \lambda^3$. When the elastomer is subject to a combination of a force $P$ and a voltage $\Phi$, both cause the elastomer to reduce thickness and increase area, such that

$$\frac{P}{LH} + \varepsilon \left(\frac{\Phi}{H}\right)^2 \lambda^3 = F(\lambda). \tag{2}$$

This equation determines the stretch caused by the combined action of the force and the voltage.

Equations (1) and (2) constitute the equations of state of the transducer, connecting the four state variables, $P, \lambda, \Phi, Q$. Once two state variables are prescribed, the other two state variables can be solved from (1) and (2). Consequently, the transducer has two degrees of freedom.

The values of these state variables are limited by mechanisms of failure. Established mechanisms of failure include material rupture, loss of tension, electrical breakdown, and electromechanical instability [16]–[20]. These mechanisms of failure are described as follows.

An elastomer may rupture if the stretch is too large. The stretch may also be limited by other considerations, such as the durability of the elastomer and the electrodes. Let the maximum stretch of operation be

$$\lambda = \lambda_{\max}. \tag{3}$$

For a dielectric elastomer transducer, it is desirable to keep the membrane in tension, as any compressive stress in the planar directions will lead to the formation of wrinkles, which may disrupt the function of the transducer. The condition for the loss of tension (LT) is

$$P = 0. \tag{4}$$

A high electric field may mobilize charged species in the dielectric elastomer, leading to localized conducting paths and finally electrical breakdown [19], [23], [26]. The electrical breakdown field $E_{\mathrm{EB}}$ may be sensitive to imperfections like voids and inclusions [27], and may depend on variables such as stretch [19], [23], [24], thickness [26], and stiffness [28]. Write the condition for electrical breakdown (EB) as

$$\Phi = E_{\mathrm{EB}} H \lambda^{-2}. \tag{5}$$

As the voltage is increased, the elastomer reduces its thickness. The positive feedback between a thinner elastomer and a higher electric field may result in electromechanical instability (EMI) [18], [29]–[31]. The condition for EMI is determined as

follows. When the applied force $P$ is held constant, the voltage $\Phi$ is a function of stretch $\lambda$, as defined by (2). The peak of the function $\Phi(\lambda)$ corresponds to the condition for EMI. Differentiate (2) with respect to $\lambda$, while holding $P$ constant and setting $d\Phi(\lambda)/d\lambda = 0$, we obtain

$$3\varepsilon \left(\frac{\Phi}{H}\right)^2 \lambda^2 = \frac{dF(\lambda)}{d\lambda}. \qquad (6)$$

This equation, together with the equations of state (1) and (2), determines the critical values of $\Phi, \lambda, Q$ for EMI under a given force $P$. It should be noted that, due to strain stiffening of the polymer at large deformation, EMI can be eliminated when $P$ is sufficiently large [32].

## III. MATERIAL MODELS

Our previous study [16] represented the stress–stretch curve by using the neo-Hookean model. Here, we represent the stress–stretch curve by using the Arruda–Boyce model [22]. The Arruda–Boyce model accounts for strain stiffening due to the finite contour length of polymer chains, which cannot be captured by the neo-Hookean model [22]. The Arruda–Boyce model describes an elastomer by using a unit cell of eight polymer chains. Let $\Lambda$ be the stretch of each polymer chain, and let $\lambda_1$, $\lambda_2$ and $\lambda_3$ be the principal stretches of the elastomer. The eight-chain model relates the stretch of the polymer chain to the stretches of the elastomer

$$\Lambda = \sqrt{\frac{\lambda_1^2 + \lambda_2^2 + \lambda_3^2}{3}}. \qquad (7)$$

Each polymer chain is modeled by a sequence of links capable of free rotation relative to each other. At a finite temperature, the relative rotations of the links allow the polymer chain to fluctuate among a large number of conformations. The statistics of the conformations gives the force-stretch behavior of the polymer chain [33]

$$\Lambda = \sqrt{n} \left(\frac{1}{\tanh \zeta} - \frac{1}{\zeta}\right) \qquad (8)$$

where $n$ is the number of links per polymer chain, and $\zeta$ is the normalized force in the polymer chain.

The Helmholtz free energy per unit volume of the elastomer is [33]

$$W = NkTn \left(\frac{\zeta}{\tanh \zeta} - 1 + \log \frac{\zeta}{\sinh \zeta}\right) \qquad (9)$$

where $kT$ is the temperature in the unit of energy, and $N$ is the number of polymer chains per unit volume of the elastomer.

For an incompressible elastomer subject to equal-biaxial stretch $\lambda$, (7) becomes

$$\Lambda = \sqrt{\frac{2\lambda^2 + \lambda^{-4}}{3}}. \qquad (10)$$

Consequently, (8)–(10) define the free-energy function $W(\lambda)$ through two intermediate variables $\Lambda$ and $\zeta$. When the stretch varies by $d\lambda$, the biaxial nominal stress $s$ does work $2sd\lambda$. This work causes the free energy to vary by $dW = 2sd\lambda$. Consequently, we obtain $s = (1/2)\, dW/d\lambda$. Recall that $s = F(\lambda)$.


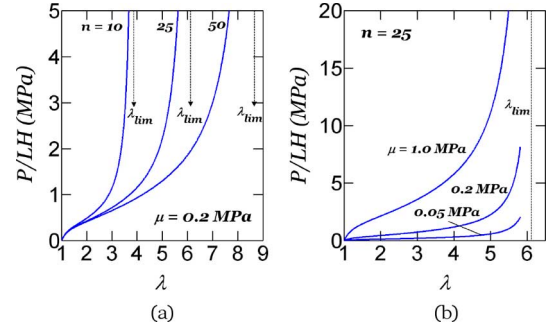
Fig. 2. Relation between stretch $\lambda$ and equal-biaxial nominal stress $P/LH$. (a) Number of links in each polymer chain $n$ sets the limit stretch $\lambda_{\text{lim}}$. (b) Small-strain modulus $\mu$ sets the amplitude of the nominal stress.
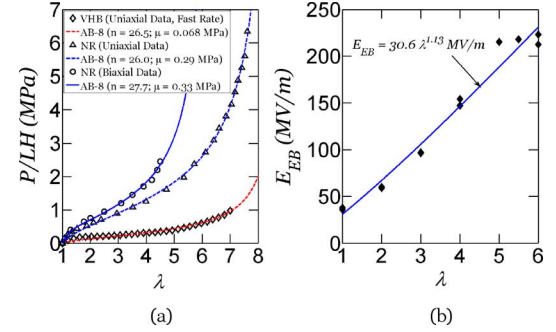


Fig. 3. (a) Experimentally measured stress–stretch curves of elastomers are fitted to the Arruda-Boyce eight-chain model (AB-8). For natural rubber [21], the data for uniaxial tension and the data for equal-biaxial tension are separately fitted. For VHB acrylic elastomer, the data for fast uniaxial tension [19] are fitted. (b) Electrical breakdown field for VHB were measured as a function of prestretch [19], [23]. The data are fitted to $E_{\text{EB}}(\lambda) = E_{\text{EB}}(1)\lambda^R$.

Calculating the derivative by using (8)–(10), we obtain

$$F(\lambda) = \frac{\sqrt{n}\mu\zeta \left(\lambda - \lambda^{-5}\right)}{3\Lambda}. \qquad (11)$$

In the absence of a voltage, the stress–stretch curve for an elastomer is given by $P/LH = F(\lambda)$. Fig. 2 plots the stress–stretch curve for the elastomer under equal-biaxial tension. In the limit $\zeta \to \infty$, each polymer chain is fully stretched, $\Lambda \to \sqrt{n}$, and the elastomer reaches the limit stretch $\lambda_{\text{lim}}$. Rewrite (10) as

$$2\lambda_{\text{lim}}^2 + \lambda_{\text{lim}}^{-4} = 3n. \qquad (12)$$

This equation determines $\lambda_{\text{lim}}$ for any given $n$. In the limit $\zeta \to 0$, the neo-Hookean model is recovered, with the small–strain shear modulus $\mu = NkT$. Note that $n$ sets the limit stretch, and $\mu$ sets the amplitude of the stress.

Fig. 3(a) fits the eight-chain model to existing experimental data for VHB under fast mechanical uniaxial loading (strain rate = 1.8 s$^{-1}$) [19], and NR under uniaxial and equal-biaxial loading [21], [22]. For NR, $n$ and $\mu$ are not significantly different when the model is fitted to uniaxial and equal-biaxial data. The maximum stretches for both VHB and NR under uniaxial stretch are similar, while the shear modulus of NR is about five times that of VHB.

In our previous study [16], the dielectric behavior is assumed to be liquid-like, such that the electrical breakdown field $E_{\text{EB}}$
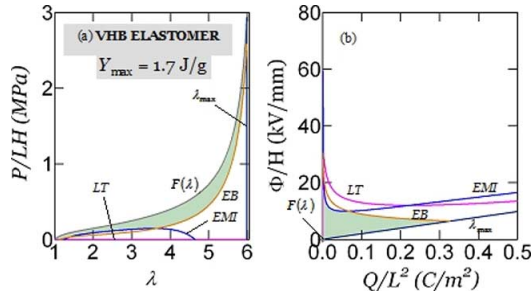
Fig. 4.    State of an elastomer is represented by a point (a) either in the stress–stretch plane, or (b) in the voltage–charge plane. Plotted on both planes are curves representing mechanisms of failure: $\lambda_{\max}$ stands for maximum stretch, EB for electrical breakdown, EMI for electromechanical instability, LT for loss of tension. Also included is the stress–stretch curve $F(\lambda)$ of the elastomer under no electric field. On the voltage–charge plane, this curve degenerates into a single point, the origin. On either plane these curves define a shaded region of allowable states. The area of the shaded region gives the theoretical maximum energy of conversion. These plots are termed *operation maps*. The two planes are constructed for VHB using available experimental data.

is constant, independent of stretch. However, experimental data on VHB dielectric elastomer shows that $E_{\mathrm{EB}}$ increases with stretch [19], [23], [24]. We fit the experimental data to

$$E_{\mathrm{EB}}(\lambda) = E_{\mathrm{EB}}(1)\lambda^{R} \qquad (13)$$

where $E_{\mathrm{EB}}(1)$ is the electrical breakdown field when the stretch is fixed at $\lambda = 1$, and $R$ is the degree of sensitivity of the electrical breakdown field toward stretch. $R = 0$ implies that the electrical breakdown field is independent of stretch. Fig. 3(b) shows equation (12) fitted to experimental data for VHB with $H = 1.0$ mm [19], [23]. This fit gives that $E_{\mathrm{EB}}(1) = 30.6$ MV/m and $R = 1.13$.

## IV. ENERGY OF CONVERSION FOR VHB AND NATURAL RUBBER

In the past decade, the VHB elastomer has been used extensively as a model material to develop actuators and generators [2]–[12], [15]–[17], [34]. As a dielectric elastomer generator, it has been shown experimentally that a VHB elastomer converts energy at a specific energy of 0.4 J/g [9]. On the other hand, NR is the most familiar elastomer, and is abundant and cheap. No research has been performed on NR in generators.

As mentioned earlier, a dielectric elastomer transducer has two degrees of freedom. We represent a state of the transducer by either a point in the stress–stretch plane [see Fig. 4(a)], or a point in the voltage–charge plane [see Fig. 4(b)]. Because the four variables $P, \lambda, \Phi, Q$ are connected through the two equations of state (1) and (2), the two planes present equivalent information in alternative forms. The two equations of state (1) and (2), in conjunction with one of (3)–(6), represent each mechanism of failure as one curve in the stress–stretch plane, and as another curve in the voltage–charge plane. Also included in the stress-stretch plane is the function $F(\lambda)$, the stress–stretch curve of the elastomer in the absence of voltage. On the voltage–charge plane, this curve degenerates into a single point, the origin. The elastomer was assumed to be stretched up to near limiting stretch in its operation.
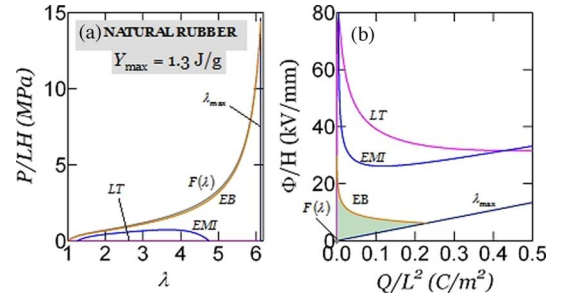


Fig. 5.    Operation maps are constructed for natural rubber using available experimental data. (a) Stress–stretch plane. (b) Voltage–charge plane.

As mentioned earlier, a point in either the stress–stretch plane or the voltage–charge plane represents a state of the transducer. Consequently, a curve in either plane represents a path of operation, a closed contour represents a cycle of operation, and the area enclosed by the contour represents the energy of conversion per cycle. By operating along the curves defined by the mechanisms of failure, the maximum energy of conversion is realized. The shaded regions in Fig. 4 define the allowable states that the dielectric elastomer transducer can operate without failure. As a generator, the cycle is described by a clockwise cycle around the shaded region on the $P$–$\lambda$ plane, and an anticlockwise cycle around the shaded region on the $\Phi$–$Q$ plane. The theoretical limit for energy of conversion is given by the area bounded by the allowable states on the work-conjugate $P$–$\lambda$ plane, or the $\Phi$–$Q$ plane. For equal-biaxial stress, neglecting dissipative effects, the shaded area on the $\Phi$–$Q$ plane is two times that in the $P$–$\lambda$ plane. For the VHB generator, the maximum energy of conversion is 1.7 J/g. One may design practical cycles within the region of allowable states. This procedure has been illustrated in a previous study [16] and will not be repeated here. We will call cycles illustrated in the stress–stretch plane or the voltage–charge plane operation maps.

Fig. 5 shows similar plots for NR. A representative value of the electrical breakdown field of NR is 30 MV/m [35], [36], comparable to that of VHB. For NR, we are unaware of any measurement of the electrical breakdown field as a function of stretch. In constructing Fig. 5, we have assumed a stretch-dependent breakdown field similar to that of VHB. For the NR generator, the maximum energy of conversion is 1.3 J/g. To further examine the effect of electrical breakdown, we will subsequently study the energy of conversion of NR for stretch-independent breakdown (see Fig 8).

It is well known that piezoelectric transducers are able to convert energy at a maximum level of 1.0 mJ/g [37], [38], subject to a strain of less than 1%. Experiments have also been conducted on electrostrictive polymers, subject to strains of about 30%, and converting energy in the region of 10 to 20 mJ/g [39]. Recent experiments conducted on dielectric elastomer generators were subject to maximum strains of about 100%, with energy of conversion between 0.1 and 400 mJ/g [9]–[12].

To ensure long-term, reliable operation, one may wish to restrict the dielectric elastomer generator within modest levels of stretch. Fig. 6 illustrates how the shaded area is affected
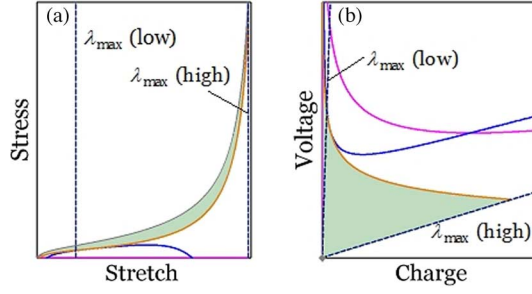
Fig. 6. Effect of the reduced maximum stretch ($\lambda_{\max}$) on the energy of conversion. The energy of conversion, given by the shaded area, is reduced due to the leftward translation of the $\lambda_{\max}$ line on the stress–stretch plane (a), and anticlockwise rotation of the same line about the origin on the voltage–charge plane (b).



Fig. 8. Maximum energy of conversion ($Y_{\max}$) as a function of operating strains ($\lambda_{\max} - 1$). For VHB, the curve is constructed by using available experimental data. For NR, two curves are constructed, one with stretch-dependent electrical breakdown field, and other with stretch-independent electrical breakdown field.
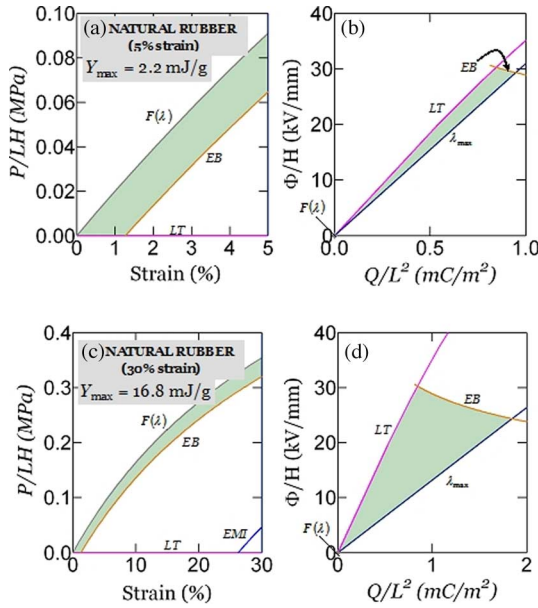


Fig. 7. Operation maps for NR when the maximum stretch is limited to 5% strain (a, b), or 30% strain (c, d).

when the maximum stretch of operation $\lambda_{\max}$ is reduced. By sweeping the $\lambda = \lambda_{\max}$ line from left to right on the $P$–$\lambda$ plane, or rotating the same line about the origin of the $\Phi$–$Q$ plane, we may visualize the maximum energy of conversion at various levels of the maximum stretch of operation.

Fig. 7 shows the allowable states when the range of operation is limited to 5% and 30% for NR. At the 5% range, both the stress–strain and voltage–charge response are approximately linear, and the energy conversion plots resemble that for a piezoelectric generator [37], [38]. For the 30% range, nonlinearity shows up. Comparing Figs. 5(a) with 7(a) and (c), and 5(b) with 7(b) and (d), we observed that the force $P$ and the charge $Q$ for small and large deformation differ by two or more orders of magnitude. As expected, the energy of conversion is 2.1 and 16.8 mJ/g for 5% and 30% strain, respectively, which is two to three orders of magnitude smaller from the potential upper bound, when the dielectric elastomer generator is stretched up to its limit. In the case where the strain is 5%, the maximum voltage gain in a contracting elastomer under open-circuit conditions
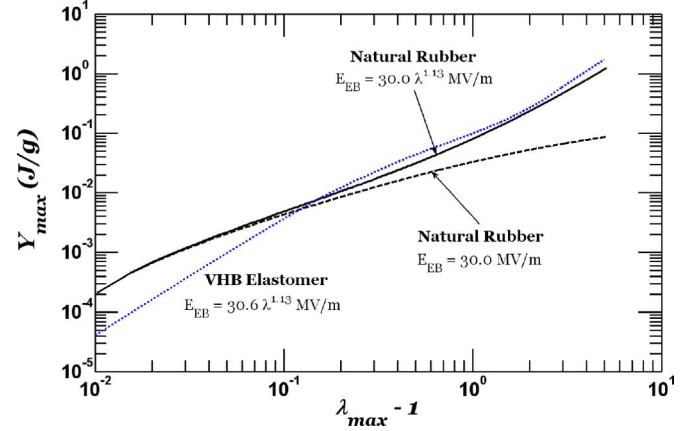
(voltage amplification) is small [<50% boost from Fig. 7(b)]. In the case where the strain is 30%, a voltage amplification up to two times is possible [>100% boost from Fig. 7(d)].

Fig. 8 demonstrates the variability of energy conversion for a dielectric elastomer generator, spanning at least 2 orders of magnitude over the entire spectrum of operating stretch. In Fig. 8, we plot the curves for VHB and NR. Due to a lack of experimental data for the dielectric strength of NR versus stretch, we assume NR with a similar stretch-dependent dielectric strength as VHB ($E_{\mathrm{EB}} = 30$ MV/m, $R = 1.13$), and NR with a stretch-independent dielectric strength, where $E_{\mathrm{EB}} = 30$ MV/m, are plotted. For strains smaller than 15%, NR outperforms VHB in terms of energy conversion. For strains above 15%, the performance of NR is comparable to VHB if they exhibit similar stretch-dependent dielectric strengths. If the dielectric strength of NR is not improved by stretching, it performs poorer as compared to VHB.

To compare with existing technologies, to achieve comparable energy of conversion as piezoceramics, we need to operate NR at 3% and VHB at 5.5% strain. To achieve that displayed by electrostrictive polymers, strains between 20% and 30% are required. Exceeding the operational strain to values above 30% gives an improved figure of merit in comparison to piezoceramics and electrostrictive polymers. Reliability issues may favor elastomer generators, even when operated at low strains, being well adapted to be used in offshore environments. Finally, it should also be noted that, although NR performs better than VHB at low strains, it is five times stiffer than VHB, which requires five times more stress to stretch.

## V. EFFECT OF MATERIAL PARAMETERS ON ENERGY OF CONVERSION

No dielectric elastomer has been designed specifically for generators. An elastomer optimized for actuators may not be optimal for generators. In anticipating efforts to design elastomers specifically for generators, we may ask: How do material parameters affect the energy of conversion?

We begin by considering the case that the operation is at small strains, due to, e.g., considerations of durability. In this case, both the stress–strain and voltage–charge relations are linear, see Fig. 7(a) and (b). Let $e = \lambda - 1$ be the strain. The line for electrical breakdown (EB) takes the form

$$\frac{P}{LH} = 6\mu e - \varepsilon E_{\mathrm{EB}}^2. \quad (14)$$

Note that the elastic modulus under equal-biaxial stretching conditions is $6\mu$. Denote the maximum strain of operation by $e_{\max}$. Inspecting Fig. 7(a), we classify materials into two types: type A ($\varepsilon E_{\mathrm{EB}}^2 < 6\mu e_{\max}$) and type B ($\varepsilon E_{\mathrm{EB}}^2 > 6\mu e_{\max}$).

For a type A material $\varepsilon E_{\mathrm{EB}}^2 < 6\mu e_{\max}$, the generator is limited partly by electrical breakdown and partly by loss of tension. The maximum energy of conversion is twice the shaded area in Fig. 7(a), namely,

$$Y_{\max} = 2e_{\max}\varepsilon E_{\mathrm{EB}}^2 - \frac{\left(\varepsilon E_{\mathrm{EB}}^2\right)^2}{6\mu}. \quad (15)$$

Observe that $Y_{\max}$ increases when $e_{\max}$ and $\mu$ increase.

For a type B material $\varepsilon E_{\mathrm{EB}}^2 > 6\mu e_{\max}$, the generator is no longer limited by electrical breakdown, but by loss of tension. The maximum energy of conversion is twice the area of the triangle below the stress–strain curve, namely,

$$Y_{\max} = 6\mu e_{\max}^2. \quad (16)$$

$Y_{\max}$ increases linearly with $\mu$, and quadratically with $e_{\max}$.

For large deformation, we assume an arbitrary nonlinear function $F(\lambda)$ that represents the nominal stress–strain curve. We shall first assume that EMI is averted at all levels of stretch, so that the allowable states are determined by $F(\lambda)$, electrical breakdown, loss of tension, and material rupture. Let $\lambda_0$ be the stretch where the EB line intersects the horizontal axis of the $P$–$\lambda$ plane. For a stretch $\lambda$ in the interval $1 < \lambda < \lambda_0$, the allowable states are bound between $F(\lambda)$ and loss of tension $P = 0$. For a stretch $\lambda$ in the interval $\lambda_0 < \lambda < \lambda_{\max}$, the allowable states are bound between $F(\lambda)$ and electrical breakdown $\Phi = E_{\mathrm{EB}}H\lambda^{-2}$. According to the equation of state (2), the force at electrical breakdown is

$$\frac{P}{LH} = F(\lambda) - \frac{\varepsilon E_{\mathrm{EB}}^2}{\lambda}. \quad (17)$$

The maximum energy of conversion is twice the shaded area in Fig. 7(c), given by

$$Y_{\max} = 2\int_1^{\lambda_0} F(\lambda)d\lambda + 2\int_{\lambda_0}^{\lambda_{\max}} \frac{\varepsilon E_{\mathrm{EB}}^2}{\lambda}d\lambda. \quad (18)$$

Substituting (13) into (18), we obtain

$$Y_{\max} = 2\int_1^{\lambda_0} F(\lambda)d\lambda + 2\varepsilon E_{\mathrm{EB}}^2 \log\left(\frac{\lambda_{\max}}{\lambda_0}\right), \quad \text{for } R = 0 \quad (19a)$$

$$Y_{\max} = 2\int_1^{\lambda_0} F(\lambda)d\lambda + \varepsilon\left[E_{\mathrm{EB}}(1)\right]^2 \left(\frac{\lambda_{\max}^{2R} - \lambda_0^{2R}}{R}\right), \quad \text{for } R \neq 0. \quad (19b)$$
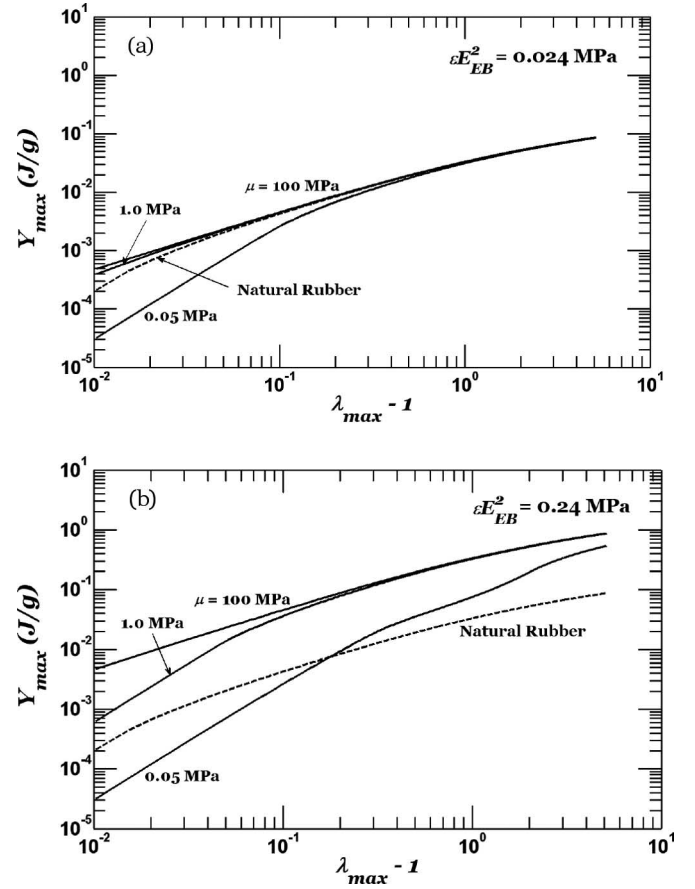


Fig. 9. Effect of material parameters $\mu$ and $\varepsilon E_{\mathrm{EB}}^2$ on the maximum energy of conversion $Y_{\max}$. Natural rubber with $E_{\mathrm{EB}} = 30.0\,\mathrm{MV/m}$ is taken as a reference (dashed lines). (a) $\varepsilon E_{\mathrm{EB}}^2 = 0.024\,\mathrm{MPa}$, a value for NR is used. (b) Value $\varepsilon E_{\mathrm{EB}}^2 = 0.24\,\mathrm{MPa}$ is used. The energy of conversion is increased by increasing $\mu$ and $\varepsilon E_{\mathrm{EB}}^2$.

Assuming that $\lambda_{\max} \gg \lambda_0$, the first term on the right-hand side is negligible. Equation (19) shows that $Y_{\max}$ again increases with $\varepsilon E_{\mathrm{EB}}^2$.

If EMI occurs over a range of stretch, the expression for $Y_{\max}$ becomes very complex. In this case, EMI cuts out a portion of the shaded area otherwise bounded by the EB boundary in a soft elastomer, resulting in a smaller $Y_{\max}$. To obtain $Y_{\max}$ for such elastomers, numerical methods must be used to compute the shaded area.

Fig. 9 shows the effect of varying $\mu$ on the maximum energy of conversion $Y_{\max}$. In this plot, $\varepsilon E_{\mathrm{EB}}^2$ is assumed to be fixed and does not vary with stretch. For the smaller value of $\varepsilon E_{\mathrm{EB}}^2 = 0.024\,\mathrm{MPa}$ [see Fig. 9(a)], taken from the properties of NR, $Y_{\max}$ saturates at small strains of operation at high $\mu$, and $Y_{\max}$ can no longer be increased further beyond $\mu = 100$ MPa for the entire range of strain of operation. Therefore, NR appears to be at an optimal stiffness for energy conversion when operating at strains $>100\%$. For small strain operation $<100\%$, marginal gains in $Y_{\max}$ can be achieved with a stiffer material.

Are there better candidates than NR for energy conversion? Based on existing experimental data, the Maxwell stress at electrical breakdown for isoprene NR was measured to be $\varepsilon E_{\mathrm{EB}}^2 =$
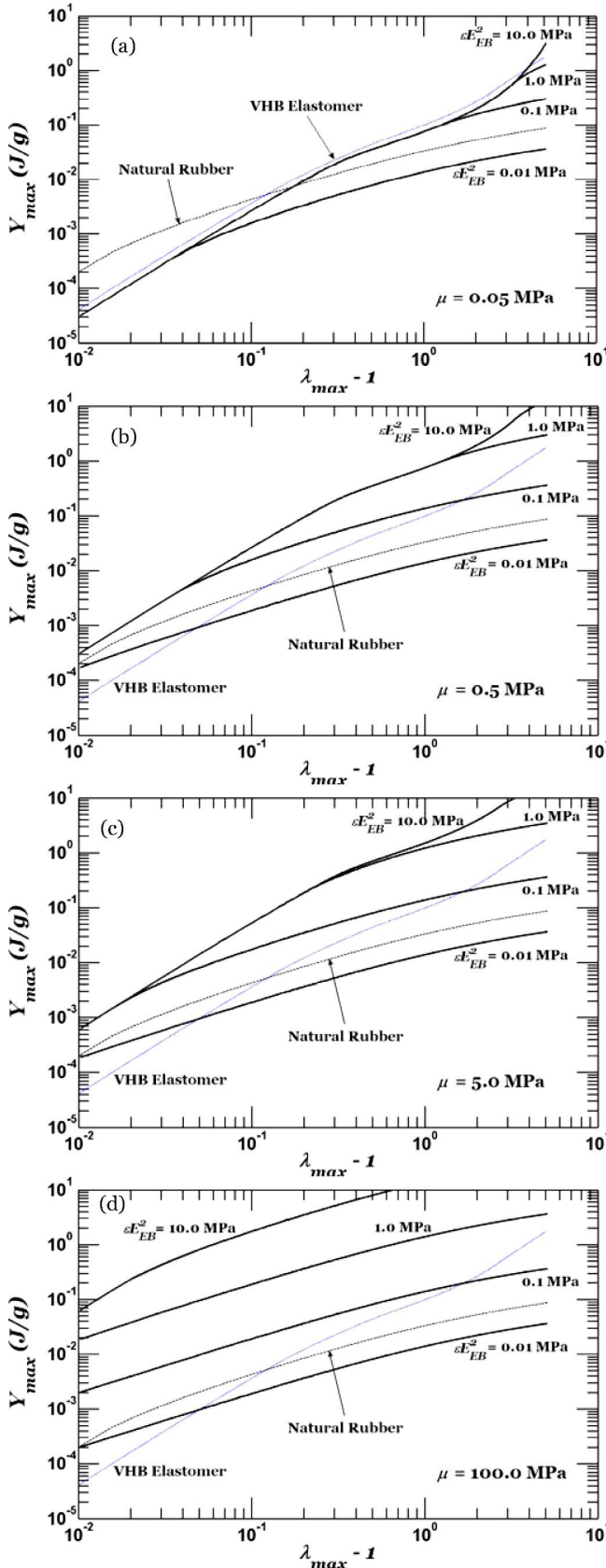
Fig. 10. Effect of material parameters $\mu$ and $\varepsilon E_{EB}^2$ on the maximum energy of conversion $Y_{max}$. NR with $E_{EB} = 30.0$ MV/m (dashed lines) and VHB (dotted lines) are taken as references. Four values of shear modulus were used: (a) $\mu = 0.05$ MPa, (b) $\mu = 0.5$ MPa, (c) $\mu = 5.0$ MPa, and (d) $\mu = 100$ MPa.

0.11 MPa, and natural muscle gives $\varepsilon E_{EB}^2 = 0.35$ MPa [34]. Hence, if $\varepsilon E_{EB}^2$ can be increased to ten times that of NR, i.e., $\varepsilon E_{EB}^2 = 0.24$ MPa [see Fig. 9(b)], $Y_{max}$ is observed to increase about an order of magnitude if $\mu \geq 1.0$ MPa. $Y_{max}$ remains relatively unchanged for the soft elastomer ($\mu = 0.05$ MPa) at strain of operation <20%, as it now fails predominantly by EMI in that region, and therefore, the full potential cannot be realized. At higher strains of operation, due to strain stiffening, the soft elastomer is able to avert EMI, resulting in gains of an order of magnitude.

What happens if $\varepsilon E_{EB}^2$ is further increased? We explore the effect of varying $\varepsilon E_{EB}^2$ over four orders of magnitude, for four different elastic moduli, as shown in Fig. 10. Also included in Fig. 10 are NR with a stretch-independent $E_{EB} = 30.0$ MV/m and VHB elastomer with stretch-dependent $E_{EB}$. Note that VHB has $\varepsilon E_{EB}^2 = 0.037$ MPa at low stretch and $\varepsilon E_{EB}^2 = 2.12$ MPa at high stretch. When the elastomer is not sufficiently stiff to avert EMI, increasing $\varepsilon E_{EB}^2$ does nothing to improve $Y_{max}$ at small to moderate strains of operation. In all cases, strain stiffening at high strains of operation improves $Y_{max}$.

## VI. CONCLUSION

We model a generator as a system of two degrees of freedom. Operation maps are constructed on both the stress-stretch plane and the voltage-charge plane. A point in such a plane represents a state of the generator, a curve represents a path of operation, a contour represents a cycle of operation, and the area enclosed by the contour represents the energy of conversion per cycle. Each mechanism of failure is represented by a curve in the plane. The curves of all the known mechanics of failure enclose the region of allowable states. The area of this region defines the maximum energy of conversion. Practical cycles can be designed within the region of allowable states. We construct operation maps for NR and VHB by using available experimental data and explore the effect of the maximum strain of operation. We further explore effects of varying material properties on the maximum energy of conversion. Following this study, experiments can be conducted to characterize various elastomers like NR and PDMS. In particular, it will be informative to know if their electrical breakdown field is stretch dependent. Mechanical and electrical losses can be quantified via experiments. Theoretical models with dissipation can also be introduced into our framework, to determine the optimal speed of operation that maximizes power. Finally, it is hoped that this approach will aid in the efforts to select and design elastomers for generators.

## REFERENCES

[1] R. A. Anderson, "Mechanical-stress in a dielectric solid from a uniform electric-field," *Phys. Rev. B*, vol. 33, no. 2, pp. 1302–1307, 1986.
[2] N. Galler, H. Ditlbacher, B. Steinberger, A. Hohenau, M. Dansachmüller, F. Camacho-Gonzales, S. Bauer, J. R. Krenn, A. Leitner, and F. R. Aussenegg, "Electrically actuated elastomers for electro-optical modulators," *Appl. Phys. B, Lasers Opt.*, vol. 85, no. 1, pp. 7–10, Oct. 2006.
[3] C. Keplinger, M. Kaltenbrunner, N. Arnold, and S. Bauer, "Capacitive extensometry for transient strain analysis of dielectric elastomer actuators," *Appl. Phys. Lett.*, vol. 92, no. 19, art. 192903, May 12, 2008.

[4] C. Keplinger, M. Kaltenbrunner, N. Arnold, and S. Bauer, "Rontgen's electrode-free elastomer actuators without electromechanical pull-in instability," *Proc. Natl. Acad. Sci. USA*, vol. 107, no. 10, pp. 4505–4510, Mar. 9, 2010.

[5] G. Kofod, M. Paajanen, and S. Bauer, "Self-organized minimum-energy structures for dielectric elastomer actuators," *Appl. Phys. A, Mater. Sci. Process.*, vol. 85, no. 2, pp. 141–143, Nov. 2006.

[6] G. Kovacs, L. Düring, S. Michel, and G. Terrasi, "Stacked dielectric elastomer actuator for tensile force transmission," *Sens. Actuators A, Phys.*, vol. 155, no. 2, pp. 299–307, Oct. 2009.

[7] R. Pelrine, R. Kornbluh, Q. Pei, and J. Joseph, "High-speed electrically actuated elastomers with strain greater than 100%," *Science*, vol. 287, no. 5454, pp. 836–839, Feb. 4, 2000.

[8] X. H. Zhao and Z. G. Suo, "Method to analyze programmable deformation of dielectric elastomer layers," *Appl. Phys. Lett.*, vol. 93, no. 25, art. 251902, Dec. 22, 2008.

[9] R. Pelrine, J. Eckerle, P. Jeuck, S. Oh, Q. Pei, and S. Stanford, "Dielectric elastomers: Generator mode fundamentals and applications," in *Proc. SPIE Electroactive Polym Actuators Devices*, vol. 4329, pp. 146–155, Mar. 2001.

[10] C. Jean-Mistral, S. Basrour, and J. J. Chaillout, "Dielectric polymer: Scavenging energy from human motion," in *Proc. SPIE Electroactive Polym. Actuators Devices*, vol. 6927, pp. 692716-1–692716-10, Mar. 2008.

[11] Y. H. Iskandarani, R. W. Jones, and E. Villumsen, "Modeling and experimental verification of a dielectric polymer energy scavenging cycle," in *Proc. SPIE Electroactive Polym Actuators Devices*, vol. 7287, art. 72871Y, Mar. 2009.

[12] S. Chiba, M. Waki, R. Kornbluh, and R. Pelrine, "Innovative power generators for energy harvesting using electroactive polymer artificial muscles," in *Proc. SPIE Electroactive Polym. Actuators Devices*, vol. 6927, art. 692715, Mar. 2008.

[13] S. R. Platt, S. Farritor, and H. Haider, "On low-frequency electric power generation with PZT ceramics," *IEEE/ASME Trans. Mechatronics*, vol. 10, no. 2, pp. 240–252, Apr. 2005.

[14] A. M. Wickenheiser, T. Reissmann, and W. J. Wu, "Modeling the effects of electromechanical coupling on energy storage through piezoelectric energy harvesting," *IEEE/ASME Trans. Mechatronics*, vol. 15, no. 3, pp. 400–411, Apr. 2010.

[15] P. Lochmatter, G. Kovacs, and M. Wissler, "Characterization of dielectric elastomer actuators based on a visco-hyperelastic film model," *Smart Mater. Struct.*, vol. 16, no. 2, pp. 477–486, Apr. 2007.

[16] S. J. A. Koh, X. H. Zhao, and Z. G. Suo, "Maximal energy that can be converted by a dielectric elastomer generator," *Appl. Phys. Lett.*, vol. 94, no. 26, art. 262902, 2009.

[17] S. J. A. Koh. "Maximal energy that can be harvested from a dielectric elastomer generator," presented at the MRS Symp. Z, Boston, MA, vol. 1218E, 2009.

[18] K. H. Stark and C. G. Garton, "Electric Strength of Irradiated Polythene," *Nature*, vol. 176, no. 4495, pp. 1225–1226, 1955.

[19] J. S. Plante and S. Dubowsky, "Large-scale failure modes of dielectric elastomer actuators," *Int. J. Solids Struct.*, vol. 43, no. 25–26, pp. 7727–7751, Dec. 2006.

[20] M. Moscardo, X. H. Zhao, Z. G. Suo, and Y. Lapusta, "On designing dielectric elastomer actuators," *J. Appl. Phys*, vol. 104, no. 9, Nov. 1, 2008.

[21] L. R. G. Treloar, *The Physics of Rubber Elasticity*. Oxford, U.K.: Clarendon, 1975, p. 101.

[22] E. M. Arruda and M. Boyce, "A three-dimensional constitutive model for the large stretch behavior of rubber elastic materials," *J. Mech. Phys. Solids*, vol. 41, no. 2, pp. 389–412, 1992.

[23] G. Kofod, "Dielectric elastomer actuators," Ph.D. thesis, Tech. Univ. Denmark, Lyngby, Denmark, Sep. 2001, p. 72.

[24] G. Kofod, R. Kornbluh, R. Pelrine, and P. Sommer-Larsen, "Actuation response of polyacrylate dielectric elastomers," *J. Int. Mater. Syst. Struct.*, vol. 14, no. 12, pp. 787–793, 2003.

[25] R. E. Pelrine, R. D. Kornbluh, and J. P. Joseph, "Electrostriction of polymer dielectrics with compliant electrodes as a means of actuation," *Sens. Actuators A*, vol. 64, no. 1, pp. 77–85, 1998.

[26] J. J. O'Dwyer, *The Theory of Dielectric Breakdown of Solids*. Oxford, U.K.: Clarendon, 1964, p. 123.

[27] J. D. Vogan, "Development of dielectric elastomer actuators for MRI devices," Master's thesis, Massachusetts Inst. Technol., Cambridge, MA, Jun. 2004, p. 15.

[28] M. Kollosche, M. Melzer, A. Becker, H. Stoyanov, D. N. McCarthy, H. Ragusch, and G. Kofod, "The influence of mechanical properties in the electrical breakdown in poly-styrene-ethylene-butadiene-styrene thermoplastic elastomer," in *Proc. SPIE Electroactive Polym. Actuators Devices*, vol. 7287, art. 728729, Mar. 2009.

[29] X. Zhao and Z. Suo, "Method to analyze electromechanical instability of dielectric elastomers," *Appl. Phys. Lett.*, vol. 91, no. 6, art. 061921, pp. 061921-1–061921-3, 2007.

[30] X. Zhao and Z. Suo, "Electromechanical instability of semi-crystalline polymers," *Appl. Phys. Lett.*, vol. 95, no. 3, art. 031904, pp. 031904-1–031904-3, 2009.

[31] A. N. Norris, "Comment on 'method to analyze electromechanical instability of dielectric elastomers'," *Appl. Phys. Lett.*, vol. 92, no. 2, art. 026101, 2008.

[32] X. Zhao, W. Hong, and Z. Suo, "Electromechanical hysteresis and coexistent states in dielectric elastomers," *Phys. Rev. B*, vol. 76, no. 13, art. 134113, 2007.

[33] W. Kuhn and F. Grün, "Beziehungen zwischen elastischen Konstanten und Dehnungs-doppelbrechung hochelastischer Stoffe," *Kolloidzschr*, vol. 101, pp. 248–271, 1942.

[34] P. Brochu and Q. Pei, "Advances in dielectric elastomers for actuators and artificial muscles," *Macromolecular Rapid Commun.*, vol. 31, no. 1, pp. 10–36, 2010.

[35] L. A. Dissado and J. C. Fothergill, *Electrical Degradation and Breakdown in Polymers*. London, U.K.: Peter Peregrinus Ltd., 1992, p. 424.

[36] D. R. Lide, *CRC Handbook of Chemistry and Physics*, 79th ed. Boca Raton, FL: CRC Press, 1998, p. 15.

[37] J. Kymissis, C. Kendall, J. Paradiso, and N. Gershenfeld, "Parasitic power harvesting in shoes," in *Dig. Second IEEE Int. Conf. Wearable Comput.*, Aug. 1998, p. 132.

[38] H. Sodano, D. Inman, and G. Park, "Comparison of piezoelectric energy harvesting devices for recharging batteries," *J. Int. Mater. Syst. Struct.*, vol. 16, no. 10, pp. 799–807, 2005.

[39] K. Ren, Y. Liu, H. Hofmann, Q. M. Zhang, and J. Blottman, "An active energy harvesting scheme with an electroactive polymer," *Appl. Phys. Lett.*, vol. 91, no. 13, art. 132910, 2007.
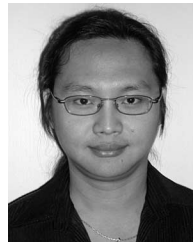
**Soo Jin Adrian Koh** was born in Singapore in 1975. He received the Ph.D. degree in integrative sciences and engineering from the National University of Singapore, Singapore, in 2008.

He is currently a Postdoctoral Fellow in the School of Engineering and Applied Sciences, Harvard University, Cambridge, MA. He is also with the Institute of High Performance Computing, Singapore. During his Ph.D. studies, he was engaged in research on modeling and simulation of mechanical properties of transition metallic nanowires. He is the author or coauthor of various papers published on the topic of metallic nanowires in *Physical Review B*, *Nanotechnology*, and *Nano Letters*. His research interests include dielectric elastomers, in particular, their usage as generators.

Dr. Koh is the recipient of the Inaugural Philip Yeo Prize, which recognizes outstanding research performed by a graduate student or Postdoctoral Fellow in Singapore.

**Christoph Keplinger** was born in Rohrbach, Austria, in 1984. He received the Master's degree in physics in 2008 from the Johannes Kepler University Linz, Linz, Austria, where he is currently working toward the Ph.D. degree in the Soft Matter Physics Department.

From 2009 to 2010, he spent six months at Harvard University on the team of Zhigang Suo to work on dielectric elastomer generators. He is also currently with the School of Engineering and Applied Sciences, Harvard University, Cambridge, MA. His current research interests include dielectric elastomers as actuators and generators.

Mr. Keplinger received the Wilhelm Macke Award for his Master's thesis.

**Tiefeng Li** was born in Hunan, China, in 1986. He received the Bachelor's degree in engineering mechanics in 2007 from Zhejiang University, Hangzhou, China, where he is currently working toward the Ph.D. degree in solid mechanics in the Institute of Applied Mechanics.

He is currently a Visiting Student at Harvard University, Cambridge, MA. He received the excellent graduation dissertation award for his Bachelor's thesis. His research interests include dielectric elastomers and ferroelectric materials.

**Zhigang Suo** was born in Xi'an, China, in 1963. He received the Bachelor's degree in engineering mechanics from Xi'an Jiaotong University, Xi'an, China, in 1985, and the Ph.D. degree in engineering sciences from Harvard University, Cambridge, MA, in 1989.

He is the Allen E. and Marilyn M. Puckett Professor of Mechanics and Materials at Harvard University. He joined the faculty of the University of California at Santa Barbara, and established a group studying the mechanics of materials and structures. The group moved to Princeton University in 1997, and to Harvard University in 2003. He was a Cofounder of iMechanica, a web of mechanics and mechanicians.

Prof. Suo is a member of the U.S. National Academy of Engineering. He is the recipient of the Humboldt Research Award. He has also received the Pi Tau Sigma Gold Medal and the Special Achievement Award for Young Investigators in Applied Mechanics, both from the American Society of Mechanical Engineers.

**Siegfried Bauer** (M'99–SM'02) was born in Karlsruhe, Germany, in 1961. He received the Master's and Ph.D. degrees in physics from the Technical University of Karlsruhe, Karlsruhe, Germany, in 1986 and 1990, respectively, and the Habilitation degree from the University of Potsdam, Potsdam, Germany, in 1996.

In 1992, he joined with the Heinrich Hertz Institute for Communication Engineering, Berlin, Germany. In 1997, he became a Professor of experimental physics at Johannes Kepler University Linz, Linz, Austria, where he has been the Head of the Soft Matter Physics Department since 2002. His current research interests include soft matter materials, which include piezo- and ferroelectrets, traditional ferroelectric polymers, and dielectric elastomers for transducer applications.

Dr. Bauer is a member of the German (DPG) and the Austrian (ÖPG) Physical Societies and of the Association of German Electrical Engineers (VDE). He received the 1993 Best Paper Award from the Information Technology Society (ITG) in the VDE, the Kurt Überreiter Award of the Berlin-Brandenburg Society of Polymer Research in 1994, the Karl Scheel Medal of the Physical Society of Berlin in 1997, and two Prize awards from the Federal Ministry of Economy of the Republic of Austria in 2007 and 2008.